PHILOSOPHICAL TRANSACTIONS OF THE ROYAL SOCIETY A MATHEMATICAL, PHYSICAL & ENGINEERING SCIENCES

The Transition to Superconductivity

P. R. Doidge

Phil. Trans. R. Soc. Lond. A 1956 **248**, 553-573
doi: 10.1098/rsta.1956.0009

THE TRANSITION TO SUPERCONDUCTIVITY

By P. R. DOIDGE*

The Royal Society Mond Laboratory, University of Cambridge

(*Communicated by D. Shoenberg, F.R.S.—Received 25 June 1955*)

CONTENTS

	PAGE
Introduction	553
The apparatus	554
Preparation of the specimens	556
General characteristics of impure specimens	556
(*a*) Electrical resistance	556
(*b*) Transition temperature	557
(*c*) Critical field curve	558
Sharpness of transitions	559
(*a*) Effect of annealing	559
(*b*) Effect of small magnetic fields	560
(*c*) Discussion	561
Measurements of transitions in a magnetic field	562
Discussion	567
(*a*) Conditions for nucleation	567
(*b*) The effect of current	571
(*c*) Relevance to existing phenomenological theories of superconductivity	572
References	573

Magnetic and electrical measurements have been made of the effect of impurity on the transitions to superconductivity in tin. Reproducible results were obtained only with well-annealed monocrystalline specimens. Solution of up to 6 % indium in pure tin decreases the electronic mean free path l from about 3×10^{-3} to 3×10^{-6} cm, and over this range magnetic measurements show that there is only a small depression of the transition temperature T_c and a small alteration in the critical field curve of H_c and T. Electrical measurements show that if $l>l_c$, where $l_c=8\times10^{-6}$ cm, the resistance transitions are sharp and almost concurrent with the magnetic transitions. However, if $l<l_c$ superconducting nucleation apparently occurs, since a state of partial superconductivity exists with zero resistance, but no exclusion of magnetic induction, in fields greater than H_c but less than H_c', where it has been found that at any one temperature $H_c/H_c'=l/l_c$. This relation describes in broad outline the dependence of H_c' on l and temperature, although the interpretation of the results is complicated by considerable broadening of the resistance transitions and the appearance of a sensitive non-linear dependence on the measuring current of the temperature of nucleation. These complicating effects may wholly or partly be due to inhomogeneities in indium concentration. The concept of a range of coherence ξ of the superconducting phase is used in formulating the thermodynamic conditions for the formation in a magnetic field of superconducting nuclei with cylindrical and spherical symmetry. It is shown that the main features of superconducting nucleation in homogeneous tin-indium alloys can be accounted for if $\xi=\dfrac{2\lambda_0 l}{l_c(1-t^2)^{\frac{1}{2}}}$, where $t=T/T_c$ and λ_0 is the penetration depth at 0°K. The implication that ξ greatly exceeds l just below T_c is supported by a consideration of the sharpness of resistance transition and the shape of the critical field curve near T_c. The formula for ξ resembles that given in Pippard's phenomenological theory of superconductivity (1953).

Introduction

The transition to superconductivity in a pure metal is very nearly discontinuous, and a sharply delineated critical field curve marks the transition from the normal state to a superconducting state in which electrical and magnetic measurements show the absence of both

* Now at Queen Mary College, University of London.

electrical resistance and magnetic induction. The behaviour of most of those alloys which are not stoichiometric compounds (summarized by Shoenberg 1952) is very different; the transitions occupy a large interval of temperature or field, normal resistance only appears in fields much larger than that which first penetrates into the alloy, and the Meissner effect is imperfectly exhibited. This behaviour has been attributed (Mendelssohn 1935) to the existence of inhomogeneities which permit the establishment, in fields greater than the usual critical field, of a sponge-like structure of superconducting sheets enclosing meshes of normal material. The possibility of superconductivity existing locally in the neighbourhood of such inhomogeneities has in turn been attributed to a negative surface energy there at a boundary between normal and superconducting phases. For certain alloys improvement of the physical purity restores the superconducting behaviour to something like that of a pure metal.

A study has been made of the gradation between the two types of behaviour shown by pure and alloyed superconductors in the particular instance of solid solutions of indium in tin. Specimens of this alloy can be made predominantly monocrystalline and homogeneous, so that there is some hope that the impure specimens only differ significantly from pure tin in respect of the electronic mean free path l of normal electrons. By making concurrent resistance and magnetic measurements it has been found that, if l is decreased below a certain critical value l_c, certain features typical of superconducting alloys are revealed which suggest the appearance of a negative surface energy encouraging superconducting nucleation; l_c is of the same order of magnitude as the penetration depth at absolute zero of a magnetic field into tin. Pippard (1951) has interpreted the surface energy in terms of an interaction within the electron assembly having a range dependent on the density of scattering centres and on the temperature, and this concept forms the basis of his phenomenological theory of superconductivity (Pippard 1953). It is shown that the present results provide strong evidence for the existence of such a range of coherence.

The apparatus

The apparatus was designed to measure concurrently, during the course of a single experiment, both the electrical resistance transitions to superconductivity in various fields and the inception of the Meissner effect in the same monocrystalline specimen; temperature is chosen as the variable in observing the transitions.

The specimen, usually a wire 9 cm long, is mounted in the appendix of a liquid helium cryostat, the temperature of which can be automatically controlled to within 10^{-4} °K during the time taken for a single measurement. The specimen is lightly attached to an insulating base by its current and potential leads which are in the form of thin copper wire helices, and is thus unstrained. Its electrical resistance is measured by means of a Kapitza–Milner (1937) potentiometer made adequately sensitive by photoelectric amplification of the galvanometer deflexions. Potential differences of 10^{-8} V developed across the specimen can be detected.

Changes of the magnetic moment of the specimen are measured ballistically. The disposition of the coils is shown schematically in figure 1; the solenoid L_s provides measuring fields; the middle part of the specimen is surrounded by a coil L_m, and this is connected to a ballistic galvanometer through two coils L_c and L_c' which are in series opposition with L_m.

Photoelectric amplification of the deflexions is available for the highest sensitivity. L_c, similar to L_m, is remote from the specimen, and L_c' is a small coil which can be set at an angle to the measuring field. There is in general a ballistic deflexion of the galvanometer when the measuring field is switched off; before an experiment this deflexion is made as small as possible by adjusting the orientation of L_c'. During an experiment at the temperature of liquid helium, a more exact balance of the magnetic fluxes through L_m and L_c with L_c' is obtained by adjusting a fraction of the solenoid (L_s) current tapped off through a trimming coil L_t which surrounds L_c. This balance is obtained with the specimen in the normal state, and holds for any measuring field. When the specimen becomes superconducting there is a ballistic deflexion θ of the galvanometer on switching off the measuring field. It is only

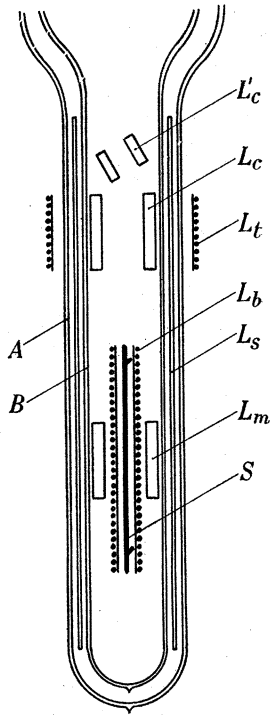

FIGURE 1. Schematic diagram showing the disposition of the coils. A and B, liquid oxygen and helium dewars; S, the specimen. The measuring coil L_m and the compensating coil L_c each have about 32000 turns, and the subsidiary compensating coil L_c' about 5000 turns of 47 s.w.g. copper wire. Together L_m, L_c and L_c' have a resistance of 22000 ohms at room temperature and 190 ohms at liquid helium temperatures. L_s, L_t and L_b are single-layer solenoids.

the magnetic flux excluded from the middle part of the specimen which determines θ, since the ends of the specimen are remote from L_m; so also are the stubs which sometimes form part of the monocrystalline specimen and to which potential leads may be attached.

The progress of a transition is described by the way in which μ decreases from unity to zero, where

$$\mu = 1 - \frac{\theta}{\theta_s}, \tag{1}$$

θ_s being the ballistic deflexion when the transition to superconductivity is apparently complete. μ will be the effective permeability of the specimen in the measuring field provided that the Meissner effect is fully exhibited when the field is switched off. A null method of measurement can also be used by balancing the moment of the specimen with that of a further coil L_b carrying a fraction of the current through L_s; L_b has the same length as the specimen and surrounds it. However, this method is only used with measuring fields less than about 10 gauss; with larger fields, the field produced by L_b in the space unoccupied by the specimen in order to compensate the excluded flux may be appreciable, and may

contribute a spurious apparent width to the magnetic transitions. The sensitivity and stability of this part of the apparatus is such that changes of μ of 0·02 can be detected in a specimen of 1 mm diameter with a measuring field of 0·1 gauss. The earth's magnetic field in the neighbourhood of the specimens is always compensated by two Helmholtz pairs of coils.

Preparation of the specimens

Tin and indium in suitable proportions are melted and mixed together *in vacuo* and then cast in Pyrex capillaries; the glass is broken off, and for some specimens potential lead stubs of the same composition are attached by local melting. The wire, about 20 cm long, is crystallized by laying it on an aluminium bar and setting up temperature gradients in the bar such that the wire first melts, and then solidifies slowly from one end. By repeating this crystallization in the opposite direction and removing about 5 cm from each end, tolerably good monocrystalline specimens are produced with a uniform concentration of indium along the length of the specimen. The specimens are then annealed *in vacuo* (it will be shown that this is an important part of the preparation) and mounted on a base by means of thin electrical leads.

In addition to these specimens of usual size, for certain investigations very small specimens have been prepared; a thin wire, bent in the form of an elongated figure eight, is crystallized from both ends, the ends are cut off, and the four arms of the resultant cross are used as current and potential leads for measuring the resistance of the small monocrystalline bead forming the intersection of the cross, of approximate size 1 mm long and 0·5 mm diameter.

General characteristics of impure specimens

(*a*) *Electrical resistance*

Electrical measurements give directly the ratio P of room temperature resistance to resistance at liquid helium temperatures, which for the normal state is almost entirely residual. The electronic mean free path l in the normal state can then be calculated from the formula

$$l = \frac{1{\cdot}05 \times 10^{-5}(\mathrm{P}-1)}{(9{\cdot}9 + 4{\cdot}4\cos^2\psi)}, \qquad (2)$$

where ψ is the angle between the tetrad axis and the direction of current flow. The angle ψ is measured by means of a goniometer after the specimen has been etched in concentrated hydrochloric acid. In deriving (2) Matthiessen's rule has been used; account has been taken of the anisotropy of the ideal resistivity (Bridgman 1928); the residual resistivity is taken as approximately isotropic (Pippard 1953); and the ratio of conductivity σ to mean free path l is taken to be $9{\cdot}5 \times 10^{10}\,\mathrm{ohm}^{-1}\,\mathrm{cm}^{-2}$ (Chambers 1952).

Figure 2 suggests that $1/l$ (calculated by means of (2) from experimental observations of P and ψ) varies approximately linearly with the atomic proportion of indium. The scatter of points probably indicates that the concentration of indium remaining in a specimen taken from the central portion of a wire which has been successively crystallized from both ends is rather less than that of the indium originally mixed with the tin, which is the concentration used as the abscissa of figure 2.

(*b*) *Transition temperature*

Figure 3 shows how the transition temperature of annealed monocrystalline specimens is depressed by the addition of indium. The transition temperature is generally here taken to be that at which $\mu = \frac{1}{2}$, and has been obtained by a small extrapolation to zero measuring

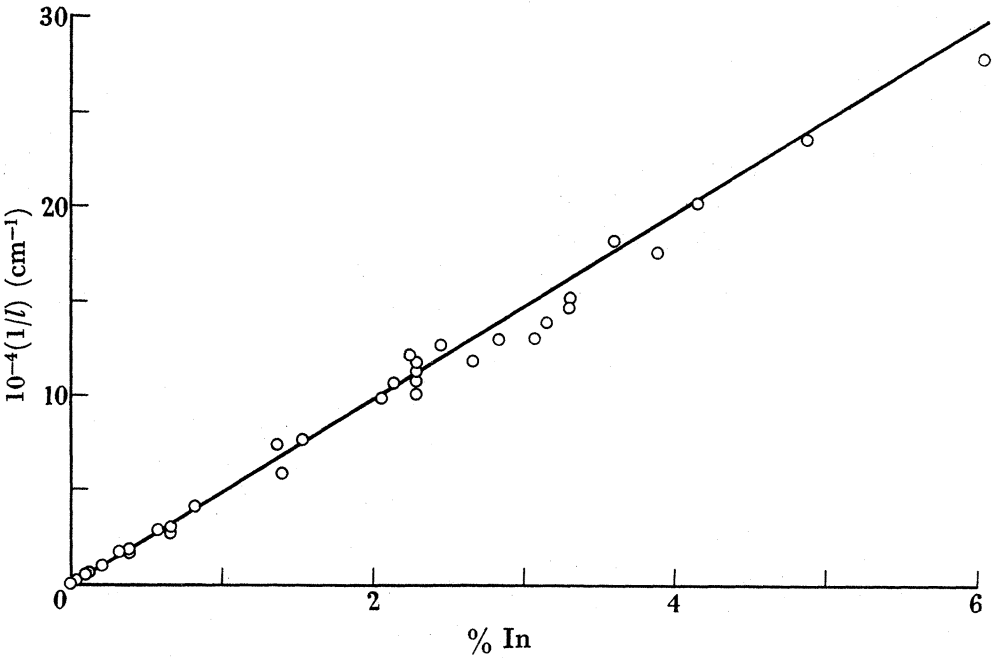

FIGURE 2. Relation between $1/l$ (derived from equation (2)) and the atomic proportion of indium dissolved in tin.

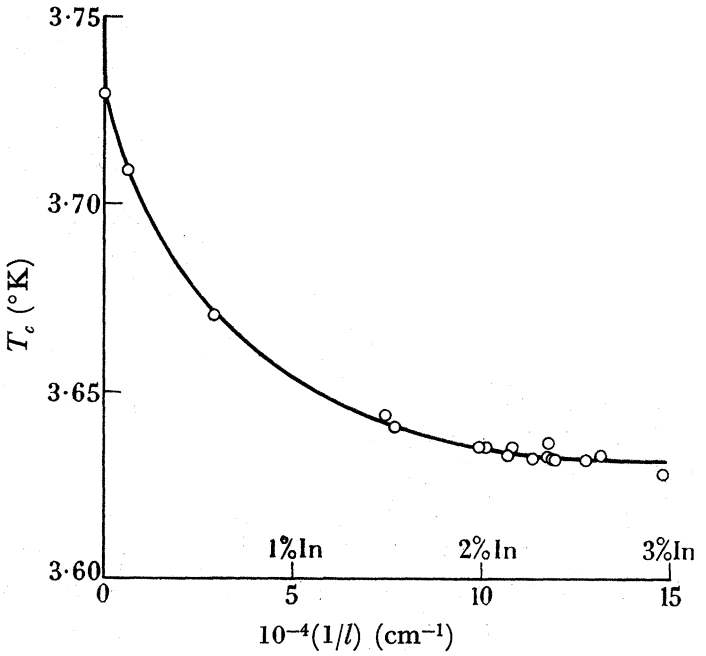

FIGURE 3. Variation of transition temperature T_c with $1/l$; the proportions of indium also shown as abscissae are derived from figure 2.

field of the transitions observed by magnetic measurements. For some of the more impure specimens represented in figure 3, which were made very small, magnetic measurements were not available; however, their electrical resistance transitions were sharp, and the transition temperature has been taken as that at which the resistance is half the residual resistance. Resistance transitions of small specimens with as much as 6 % In, although broad and not permitting a precise determination of their transition temperatures, took place over the range 3·67 to 3·63° K.

(*c*) *Critical field curve*

Another quantity which is only slightly influenced by addition of impurity is the critical field which destroys full superconductivity. Magnetic measurements on annealed monocrystalline specimens over the rather limited range of 0 to 120 G (and correspondingly 3·7 to 2·8° K) have shown that the shape of the critical field curve for an impure specimen is

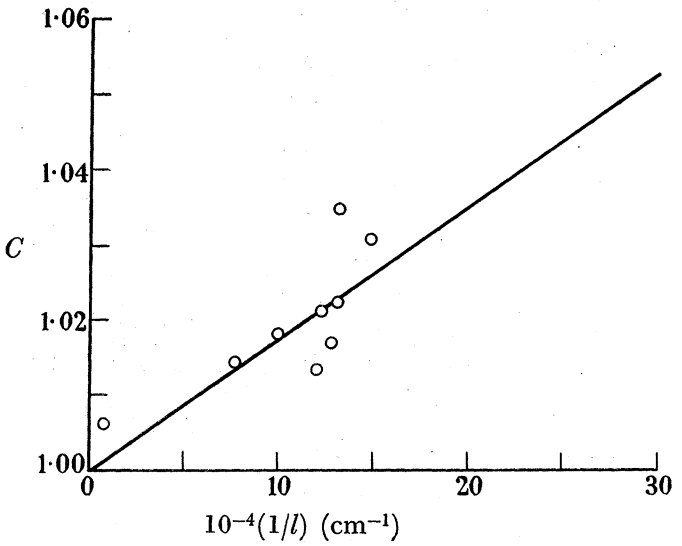

FIGURE 4. Variation with $1/l$ of the scaling factor C defined by equation (3).

not significantly different from that for pure tin as determined by Lock, Pippard & Shoenberg (1951), and a scaling factor C can be defined for the critical field curve of any one specimen

$$\frac{(H_c)_{\text{Sn-In}}}{(H_c)_{\text{Sn}}} = C\frac{(T_c)_{\text{Sn-In}}}{(T_c)_{\text{Sn}}}, \tag{3}$$

where $(T_c)_{\text{Sn}}$ and $(T_c)_{\text{Sn-In}}$ are the transition temperatures, and $(H_c)_{\text{Sn}}$ and $(H_c)_{\text{Sn-In}}$ are the critical fields measured at the same reduced temperature $t\,(=T/T_c)$, of pure and impure tin respectively. The factor C tends to increase slightly with addition of impurity, as shown in figure 4, a tendency which is there represented by a straight line with perhaps more precision than the reproducibility of the results justifies. If investigation over a much fuller range of temperature were to confirm the existence of a scaling factor C as in (3), it would follow thermodynamically (Kok 1934) that alloys of tin and indium have an electronic specific heat C^2 greater than that of pure tin.

Sharpness of transitions

(*a*) *Effect of annealing*

Impure polycrystalline specimens have resistance transitions to superconductivity in the absence of a field which sometimes occupy as large an interval of temperature as 0·1° K. The transitions of single crystals are usually sharper, but the most profound effect on the transitions is brought about by protracted annealing of crystallized specimens 10 or 15° C below their melting-points (about 230° C). Specimen 1 was investigated in detail; it was mounted so that the specimen, its base and electrical leads together could be taken out of the cryostat after an experiment at liquid helium temperatures, then sealed off in an evacuated glass tube and annealed, and afterwards replaced in the cryostat without any danger of straining the specimen. It can be seen from figure 5 that the effect of annealing

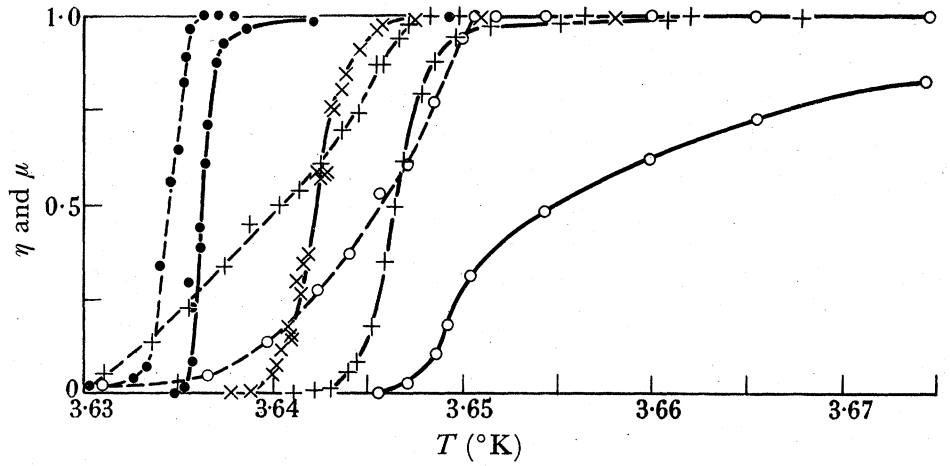

Figure 5. Effect of annealing specimen 1 (2·28 atomic % In). ——, Resistance transitions (η and T); – – – –, magnetic transitions (μ and T) extrapolated to zero measuring fields; ○, before annealing; +, after 3 h; ×, after 11½ h, ●, after 249 h of annealing at 220° C.

specimen 1 is to make the transitions, especially the resistance transitions, much sharper, and at the same time to lower the temperature at which they proceed. A comparatively short time of annealing suffices to make the resistance transition sharp, but a long time is needed before both transitions become really sharp and nearly coincident. There is no indication that the changes are complete even after 10 days' annealing.

The gap between the resistance and the magnetic transitions exemplified in figure 5 is most pronounced in specimens which are not annealed; the significant features are that the magnetic transition proceeds over a smaller and lower temperature range than does the resistance transition, and that there exists a temperature range (of variable extent according to the specimen) in which the electrical resistance begins to fall before there is any measurable appearance of diamagnetism.

It was found that annealing was accompanied by a progressive increase in the residual resistance; after 249 h this increase for specimen 1 was 12 %.

In order to find out how sharp it is possible to make the transition to superconductivity in the absence of a field, some very small annealed monocrystalline specimens were pre-

pared, in the manner previously described, in the belief that they would be more homogeneous than the specimens of usual length. Their small size and irregular shape precluded the possibility of useful magnetic measurements in small fields. Table 1 gives a summary of these and other results, selected from measurements on sixty-eight specimens; the '$\frac{1}{2}$-width' $\Delta T_{\frac{1}{2}}$ of a transition has arbitrarily been defined as the interval of temperature in which η (the ratio of resistance to residual resistance) or μ drops from $\frac{3}{4}$ to $\frac{1}{4}$. Specimens 10, 11 and 12 were very small specimens; the remainder were of normal length. Resistance transitions almost as sharp as that of pure tin (specimen 7) were obtained with specimens (1, 5, 9, 10 and 11) containing more than 2 % In. Transitions of the most impure specimens (with up to 6 % In) were comparatively broad, but showed no regular development of width or shape with increasing impurity.

TABLE 1

specimen no.	ψ	atomic % In	measured $\frac{1}{2}$-width of resistance transition	measured $\frac{1}{2}$-width of magnetic transition	$\frac{1}{2}$-width of fitted curve eq. (4)	ξ_c (cm $\times 10^{-6}$)	l (cm $\times 10^{-6}$)
7	50°	0	0·0004	0·0003	0·0005	60	3300
8	72°	0·57	0·0012	0·0010	0·0015	29	35
9	87°	2·05	0·0010	0·0005	0·0021	23	10·1
1	88°	2·28	0·0009	0·0011	0·0015	29	9·9
5	85°	2·13	0·0008	0·0007	0·0017	26	9·4
10	73°	2·28	0·0004	—	0·0004	70	8·8
11	61°	2·28	0·0007	—	0·0017	26	8·5
3	90°	2·44	0·0009	0·0034	0·0607	2·5	7·8
12	65°	6·03	0·0126	—	0·0244	4·5	3·5

(*b*) *Effect of small magnetic fields*

Measurements on specimens with about 2 % In have shown that fields of the order of 1 G or less produce no appreciable change in shape of either the resistance or magnetic transitions. Figure 6 shows that, for small fields, the depression of the temperature of resistance transition in a typical impure specimen is proportional to the applied field, and that there is thus no detectable anomalous behaviour.

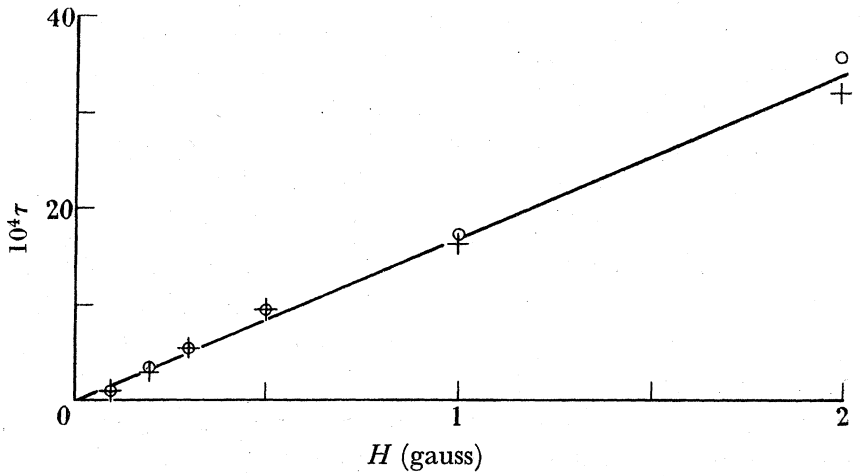

FIGURE 6. Dependence on small magnetic fields H of the depression τ of the reduced temperature ($\tau = 1-(T/T_c)$) at which: ○, $\eta = 0{\cdot}1$; +, $\eta = 0{\cdot}9$. Specimen 5 ($l = 9{\cdot}4 \times 10^{-6}$ cm).

(c) *Discussion*

The progress of the resistance transition before the appearance of any appreciable diamagnetism in a monocrystalline specimen which is not yet annealed (figure 5) suggests that certain regions prematurely become superconducting and are small enough to permit almost complete penetration of a magnetic field. The effect of annealing would be to even out these inhomogeneities. One possible explanation is that inhomogeneities in indium concentration of large amplitude and small size may exist in a crystallized specimen, and the variation of transition temperature with impurity (figure 3) is such that those regions deficient in indium would first become superconducting. Annealing would tend to even out the inhomogeneities by encouraging solid diffusion, producing sharper resistance transitions taking place at a lower mean temperature (because of the non-linearity of the curve in figure 3), and also producing an increase in residual resistance; all of these effects are observed.

The results displayed in table 1 show that transitions as sharp as any that have been observed in pure superconductors (de Haas & Voogd 1931) can be exhibited by specimens with more than 2 % impurity, and with a mean free path as small as 10^{-5} cm. The sharpness of the second-order transition to superconductivity in the absence of a field has been adduced as supporting evidence for the existence of a long-range order or coherence of the electronic configuration of the superconducting phase (Pippard 1950). If thermal fluctuations alone are responsible for the appearance of superconductivity at mean temperatures greater than T_c in spherical regions as small as but no smaller than v in volume in a perfectly homogeneous specimen, then according to Pippard the shape of the upper part of the resistance transition should take the form

$$\eta = \frac{1-\frac{1}{\sqrt{\pi}}\operatorname{Erfc}(\gamma\Delta T)}{1+\frac{2}{\sqrt{\pi}}\operatorname{Erfc}(\gamma\Delta T)}, \tag{4}$$

where $\operatorname{Erfc} x = \int_x^\infty e^{-y^2}dy$, $\Delta T = T - T_c$, $\gamma = \sqrt{\frac{c_n v}{2kT^2}}$, T is the temperature, T_c is the transition temperature, c_n is the specific heat per unit volume of the normal phase and k is Boltzmann's constant. It follows that the radius ξ_c of the spherical volume v is given in terms of the $\frac{1}{2}$-width $\Delta T_{\frac{1}{2}}$ of the transition (4) by the expression

$$\xi_c = 1{\cdot}072\left(\frac{kT^2}{\pi c_n \Delta T_{\frac{1}{2}}^2}\right)^{\frac{1}{3}}. \tag{5}$$

Sigmoid curves (4) have been fitted to those parts of the sharpest resistance transitions for which $0{\cdot}75<\eta<1$, a range in which magnetic measurements show that there is no appearance of diamagnetism and in which there should thus be a sufficiently sparse distribution of superconducting regions for (4) to be valid. In table 1 are listed the $\frac{1}{2}$-widths of the fitted curves (4) and values of ξ_c deduced by using (5). If the widths of transition are due solely to temperature fluctuations, these values of ξ_c, being the radii of the smallest superconducting regions that can be formed, should be measures of the range of coherence of the superconducting phase at the transition temperature. However, in view of the effect

of annealing shown in figure 5, it seems probable that what little width of transition remains after about 10 days' annealing is still predominantly due to inhomogeneities of the specimens, and that thermal fluctuations may not even be a major cause of transition width. Accordingly, it is permissible to regard the value of ξ_c deduced from the sharpest observed transition (that of specimen 10) as giving a minimum estimate of the range of coherence at the transition temperature, which from table 1 is seen to be at least 8 times greater than the mean free path l. This deduction has been made only for a specimen with a mean free path of about 10^{-5} cm, and may not be true for pure tin.

An even higher estimate of the minimum value of ξ_c can be deduced from the observation that the depression τ of the reduced temperature of resistance transition ($\tau = 1 - T/T_c$) is proportional to a small applied field H (figure 6). It will be shown later (footnote to p. 570) that if a specimen initially becomes superconducting in regions of radius ξ_c, then over a limited range of temperature just below the transition temperature there should exist a quadratic relation between τ and H

$$\tau = \frac{\xi_c^2 H^2}{8\lambda_0^2 H_0^2}, \tag{6}$$

where λ_0 and H_0 are the penetration depth and critical field at absolute zero. Figure 6 shows that for specimen 5 ($l = 9{\cdot}4 \times 10^{-6}$ cm) there is no clear evidence for a quadratic relation even with $H = 0{\cdot}1$ G, and $\tau = 1{\cdot}8 \times 10^{-4}$; by substituting these values into (6) it can be deduced that ξ_c, if it exists, must be greater than 6×10^{-4} cm, or more than 60 times greater than the mean free path l.

Measurements of transitions in a magnetic field

Concurrent electrical and magnetic measurements of transitions in various fields up to 120 G applied longitudinally have been made on eight annealed monocrystalline specimens of usual length containing up to 3·3 % In. The superconducting magnetic behaviour of all these specimens was found to be not much different from that of pure tin, as is apparent from the critical field data shown in figure 4. On the other hand, the character of the resistance transitions begins to change radically with the addition of more than about 2% In

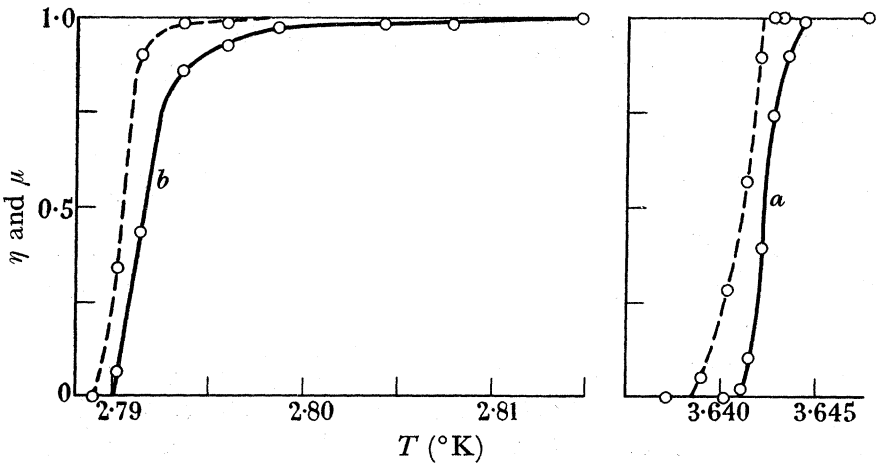

Figure 7. ——, Resistance; – – – –, magnetic transitions of specimen 2 ($l = 1{\cdot}30 \times 10^{-5}$ cm). (a) in zero field, (b) in 116·3 G.

impurity; different stages in the development of this behaviour are shown in figures 7 to 9. Specimen 2 (1·53 % In; $l = 1{\cdot}30 \times 10^{-5}$ cm) has resistance and magnetic transitions almost as sharp as those of pure tin; the resistance transition of specimen 3 (2·44 % In; $l = 7{\cdot}8 \times 10^{-6}$ cm) is for the most part sharp in the absence of a field, but becomes broader in the

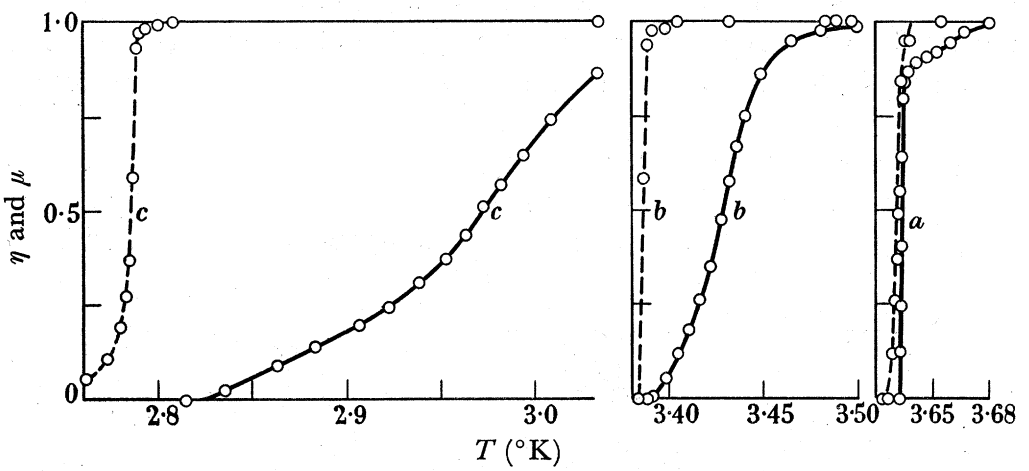

FIGURE 8. ——, Resistance; – – – –, magnetic transitions of specimen 3 ($l = 7{\cdot}8 \times 10^{-6}$ cm). (*a*) in zero field, (*b*) in 36·5 G, (*c*) in 115·4 G.

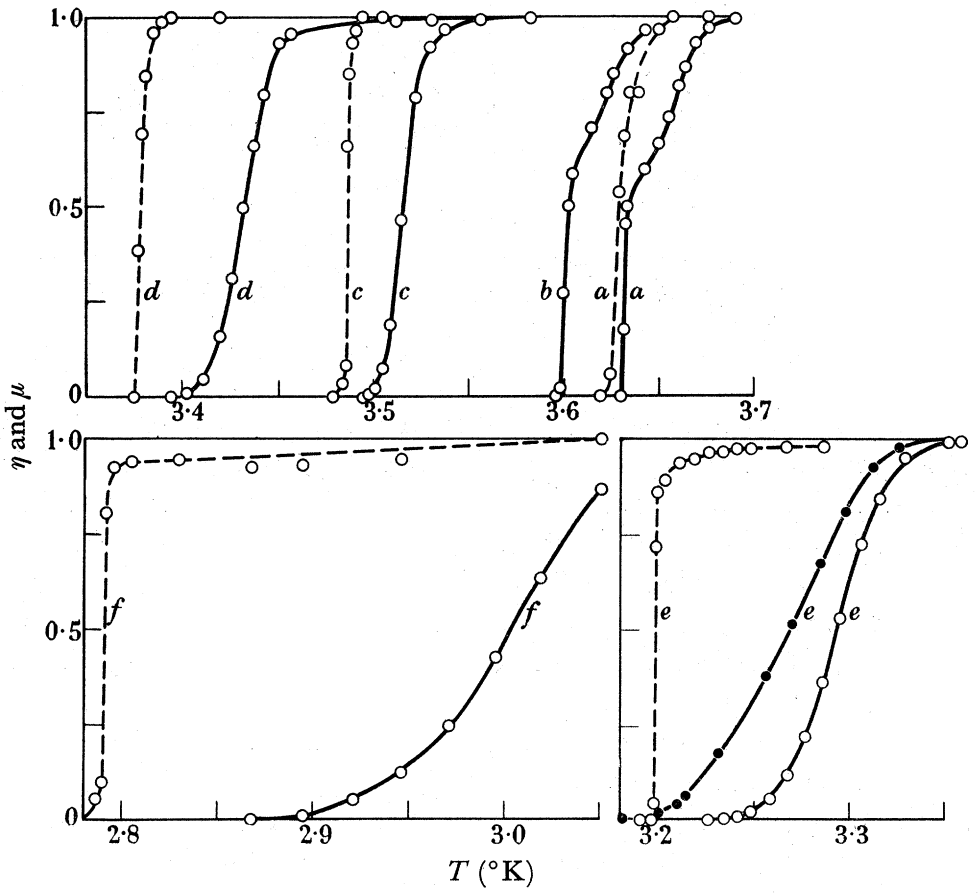

FIGURE 9. ——, Resistance; – – – –, magnetic transitions of specimen 4 ($l = 6{\cdot}8 \times 10^{-6}$ cm). (*a*) in zero field, (*b*) in 5·5 G, (*c*) in 21·8 G, (*d*) in 37·5 G, (*e*) in 62·9 G (●, applied transversely), (*f*) in 115·8 G.

presence of a field, and is completed before the inception of the magnetic transition. The separation in temperature of the resistance and magnetic transitions is most pronounced for specimen 4 (3·29 % In; $l = 6{\cdot}8 \times 10^{-6}$ cm), and, in addition, the resistance transition in the absence of a field proceeds gradually until what appears to be the true transition temperature is reached, when resistance suddenly vanishes.

The resistance transition in a transverse field of 62·9 G has also been measured for this specimen (figure 9); it is broader than that in a longitudinal field, and proceeds at lower temperatures.

For the specimens which have been investigated, the width of resistance transition does not develop regularly with increasing impurity, but for a particular specimen it does increase regularly with increasing magnetic field. No hysteresis is observed in the resistance transitions.

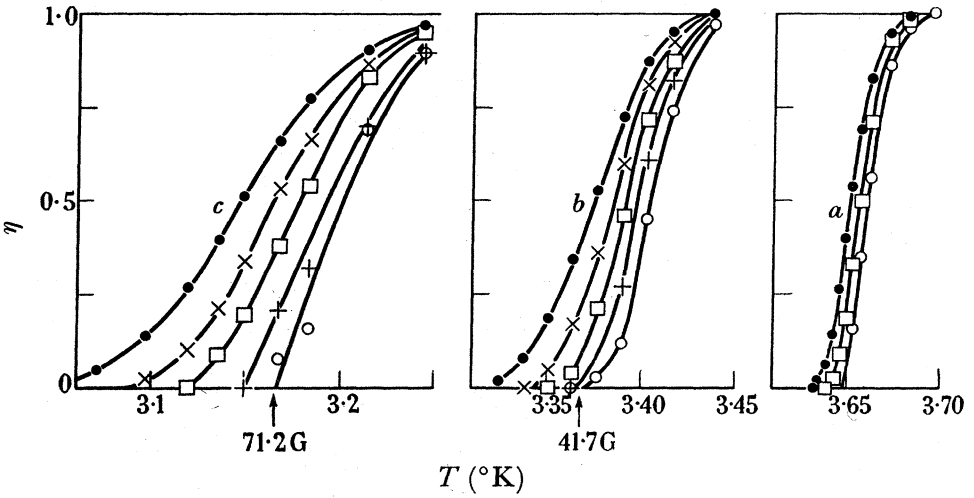

FIGURE 10. Effect of current on the resistance transitions of specimen 6 ($l = 4{\cdot}2 \times 10^{-6}$ cm). ○, 1·5 mA; +, 4 mA; □, 10 mA; ×, 20 mA; ●, 40 mA. (*a*) in zero field, (*b*) in 61·3 G, (*c*) in 113·9 G.

The greater part of each magnetic transition is accomplished within a very narrow interval of temperature, thus permitting a definition of the true temperature of transition within close limits. However, at temperatures above and below the temperature of transition there is often a certain irreproducibility of the ballistic deflexions of the galvanometer from which values of μ are calculated from (1); such deflexions are also to a small extent dependent on the conditions of field and temperature prior to the measurement. These effects are probably due to an imperfect and variable Meissner effect exhibited by these impure specimens, although with the present method of measurement it is not definitely known whether to ascribe this behaviour to the initial state of the specimen or to the final state after removal of the measuring field.

Some of the resistance transitions measured in various fields with various currents of one of a series of seven very small specimens, prepared as described previously, are shown in figure 10 (specimen 6; 4·86 % In; $l = 4{\cdot}2 \times 10^{-6}$ cm). These specimens were made small enough for the linear dimensions of the part measured to be of the same order of magnitude as the range of solid diffusion of indium in tin for the greatest practicable temperature and

period of annealing. In this way there was some hope of obtaining specimens with a reasonably even concentration of indium. The small size and irregular shape of these specimens rendered them unsuitable for magnetic measurements; however, the critical fields marked on the temperature axis of figure 10 are obtained by using the linear extrapolation of the scaling factor C shown in figure 4. It is clear that the resistance transitions of specimen 6 proceed at temperatures well above those at which the magnetic transitions would be expected to occur. Consequently the penetration of magnetic flux is complete at these temperatures, and the magnetic field is undistorted.

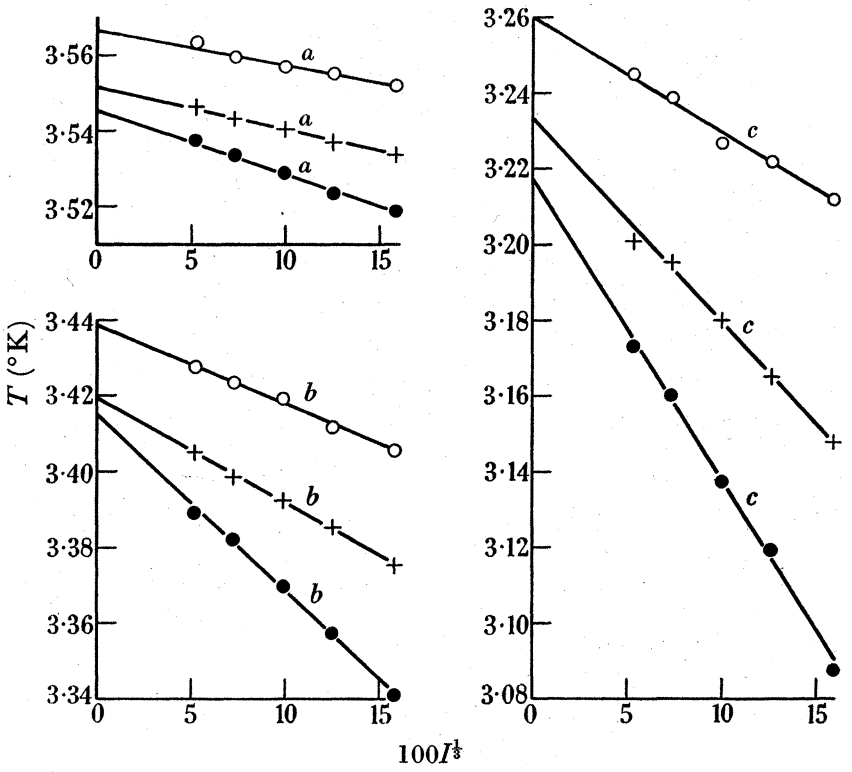

FIGURE 11. Dependence on $I^{\frac{1}{3}}$ (I = current in e.m.u.) of the temperature at which η takes certain values during the resistance transitions of specimen 6 ($l = 4{\cdot}2 \times 10^{-6}$ cm). (a) in 23·3 G, (b) in 61·3 G, (c) in 113·9 G. ○, $\eta = 0{\cdot}9$; +, $\eta = 0{\cdot}5$; ●, $\eta = 0{\cdot}1$.

There is a sensitive non-linear dependence of the temperature of resistance transition on the measuring current. This effect occurs in all specimens sufficiently impure for there to be a separation of the resistance and magnetic transitions, and in nearly all instances a simple description can be given:

$$\Delta T = KJ^{\frac{1}{3}}, \tag{7}$$

where ΔT is the depression of the temperature at which η takes a particular value, produced by a current density J e.m.u. cm^{-2}. Figure 11 shows the degree of validity of this relationship for specimen 6. The factor of proportionality K has been evaluated from the gradients of such lines as are shown in figure 11 and from rough measurements of the areas of cross-section of the specimens. The mean values of K are given in table 2; they are subject to r.m.s. deviations among the specimens of about ± 30 %. There is no regular variation of K with impurity.

From table 2 it can be seen that there is a pronounced increase of K with increasing field, and consequently with lower temperature; there is also a tendency for the lower parts of the transitions (small η) to be affected by current more than the upper parts.

In the subsequent presentation of the results extrapolation to zero current is made by application of (7) whenever sufficient data exist; without inquiring at this stage into the reason for the effect of current, this is the most obvious empirical procedure.

TABLE 2

field (gauss)	0	23	60	115
K at $\eta = 0{\cdot}9$	0·011	0·008	0·021	0·033
K at $\eta = 0{\cdot}5$	0·013	0·012	0·042	0·094
K at $\eta = 0{\cdot}1$	0·013	0·017	0·047	0·093

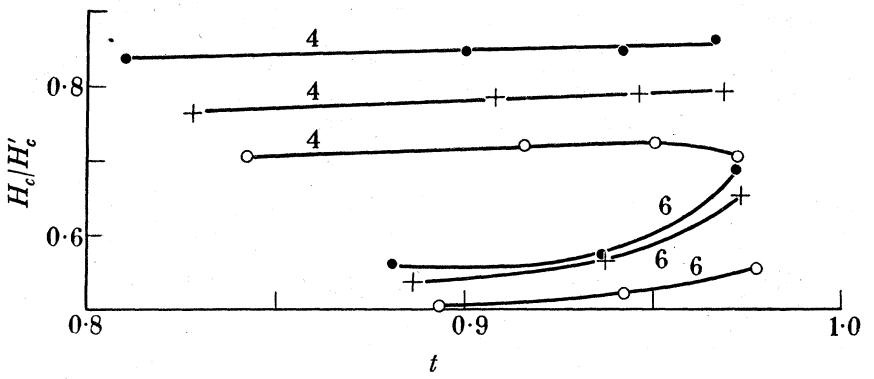

FIGURE 12. Dependence on the reduced temperature t ($t = T/T_c$) of H_c/H_c' for specimens 4 ($l = 6{\cdot}8 \times 10^{-6}$ cm) and 6 ($l = 4{\cdot}2 \times 10^{-6}$ cm). ○, $\eta = 0{\cdot}9$; +, $\eta = 0{\cdot}5$; ●, $\eta = 0{\cdot}1$.

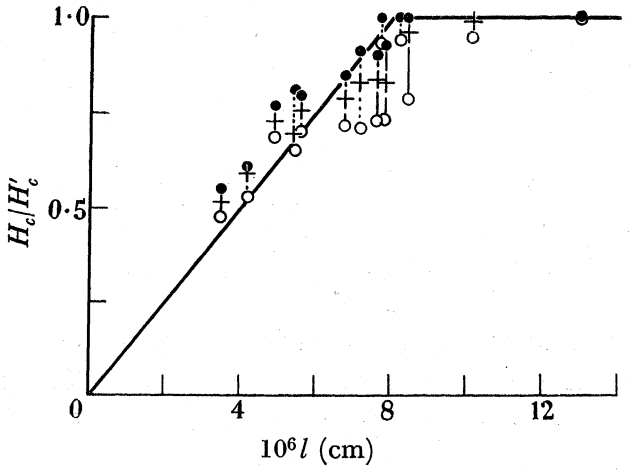

FIGURE 13. Dependence of average values of H_c/H_c' on the electronic mean free path l. ○, $\eta = 0{\cdot}9$; +, $\eta = 0{\cdot}5$; ●, $\eta = 0{\cdot}1$. Points joined by erect dotted lines are for very small specimens, for which extrapolation of resistance transitions has been made to zero measuring current. Points joined by erect full lines are for specimens of normal length.

Figure 12 shows the dependence on the reduced temperature t of H_c/H_c' for specimens 4 and 6, where H_c' is the field at which η takes a particular value during a resistance transition, and H_c is the true critical field at the same temperature. H_c is calculated by means of (3)

using a value of C taken from the straight line of figure 4. H_c/H_c' is approximately independent of t for specimen 4 ($l = 6{\cdot}8 \times 10^{-6}$ cm), and this behaviour is typical of all but the most impure specimens. Specimen 6 ($l = 4{\cdot}2 \times 10^{-6}$ cm) is an extreme example of a very impure specimen for which H_c/H_c' increases towards the transition temperature. Average values of H_c/H_c' for the various specimens are shown as a function of l in figure 13, in which values taken at $\eta = 0{\cdot}1$, $0{\cdot}5$ and $0{\cdot}9$ for each specimen are joined by erect lines. The general pattern of behaviour is that above a certain critical mean free path l_c ($l_c = 8{\cdot}0 \times 10^{-6}$ cm approximately) there is no separation of the resistance and magnetic transitions, but below l_c

$$\frac{H_c}{H_c'} = \frac{l}{l_c}. \tag{8}$$

It will be shown that the irreproducibility in detail of the results may be due to inhomogeneities in impurity concentration over any one specimen, and that some such relation as (8) would probably be obeyed by perfectly homogeneous specimens.

Discussion

(*a*) *Conditions for nucleation*

The results show that a large-scale separation of the electrical resistance and magnetic transitions begins to take place at a fairly well-defined critical impurity at which l is rather less than 10^{-5} cm; this separation is accompanied by a great increase in the width of the resistance transition and by the appearance of a sensitivity to current. At first sight it might be supposed that these effects are due to the separation of a different tin-indium phase; however, there is no suggestion of a discontinuity in the linear variation of residual resistance with impurity (as can be seen from figure 2) such as has been observed at the limit of solid solubility by Serin & Lohman (1954). Moreover, a specimen containing 16 % In, a concentration for which the phase adjacent to the solid solution in the phase diagram is stable below 100° C, was found to be superconducting throughout the range of measurement in liquid helium (below 4·2° K). It seems probable, therefore, that any separation of this phase would merely produce certain regions which would be superconducting throughout the range of temperature investigated here.

Thus it is probably significant that some of the features characteristic of the behaviour of superconducting alloys are manifested if l is diminished below a critical value l_c which is approximately equal to the penetration depth at absolute zero, λ_0, of a magnetic field into these alloys. Pippard (1951, 1955) has shown that the apparent surface energy between normal and superconducting phases is probably related to the difference (roughly speaking) between the range of coherence ξ of the superconducting phase and the penetration depth λ; a negative surface energy is possible if ξ is less than λ, in which case the formation of a large number of interphase surfaces is encouraged, and it should be possible for a finely divided structure of normal and superconducting regions to exist under conditions of field and temperature for which full superconductivity is unstable. An account of the behaviour of specimens such as number 4 (figure 9) can be given in terms of such a mixed structure provided that this allows almost complete penetration of magnetic induction. Because the specimens show a substantial Meissner effect, and little evidence of hysteresis, there is no need to assume that the structure of superconducting regions is multiply connected to any

great extent; it is therefore reasonable to start by considering the thermodynamic conditions for the formation in a magnetic field of an individual superconducting nucleus which is supposed to comprise a unit of the whole structure. It is more illuminating to introduce the concept of the range of coherence ξ than to use the interphase surface energy explicitly.

We shall consider the thermodynamic stability first of a cylindrically symmetrical filamentary superconducting nucleus in which the degree of order ω is supposed to be capable of a radial variation of the form

$$\omega = \omega_0 f\left(\frac{r}{\xi}\right), \tag{9}$$

where r is the radial distance from the axis of the nucleus, and f is a function, unspecified as yet, and subject only to the conditions $f(0) = 1$, $f'(0) = 0$ and $f(\infty) = 0$. The degree of order ω is usually identified with n_s/n_{s0}, the density of superconducting electrons expressed as a fraction of the density at 0° K.

The difference in free energy per unit volume in the absence of a field of the superconducting and normal states can be expressed as a power series in ω, as for any phase transition of the second order;

$$f_s(\omega, 0) - f_n = -\alpha\omega + \frac{\beta}{2}\omega^2 + \ldots, \tag{10}$$

where α and β are coefficients dependent on the temperature. It is assumed for the present that the free energy F_s of unit length of a nucleus in which ω varies spatially can be obtained by a volume integration of this expression without the addition of any term dependent on the gradient of ω. In the presence of a magnetic field H the appropriate thermodynamic potential of unit length of a nucleus is the Gibbs function (Pippard 1952)

$$G_s(\omega, H) = F_s(\omega, 0) - \tfrac{1}{2}MH, \tag{11}$$

where M is the magnetic moment per unit length of the nucleus.

In order to calculate M, the relation between ω, the supercurrent $\mathbf{j}_s$ and the local magnetic field $\mathbf{h}$ must be known. The London electrodynamic equation $\operatorname{curl} \Lambda\mathbf{j}_s + \mathbf{h} = 0$ can be put in the form

$$\Lambda\mathbf{j}_s + \mathbf{A} = 0, \tag{12}$$

where $\mathbf{A}$ is the magnetic vector potential, suitably gauged. In the microscopic interpretation of the London equation $\Lambda = m/n_s e^2$, where m is the effective electronic mass. This can be written in the form

$$\Lambda = \frac{n_{s0}}{n_s}\frac{m}{n_{s0}e^2} = \frac{4\pi\lambda_0^2}{\omega}, \tag{13}$$

where λ_0 is the penetration depth at 0° K; (12) can now be written

$$\mathbf{j}_s = -\frac{\omega}{4\pi\lambda_0^2}\mathbf{A}, \tag{14}$$

and this local relationship forms the basis of the present calculation.

The axis of the nucleus is assumed to be parallel to the applied field $\mathbf{H}$, in which case $\mathbf{A}$ and $\mathbf{j}_s$ are tangential. As a first approximation $\mathbf{A}$ may be assumed to have the magnitude $\frac{1}{2}Hr$, whence $\mathbf{j}_s$ and M, the magnetic moment per unit length of the nucleus, may be cal-

culated from (9) and (14). This result is readily refined by successive approximation to give M as a power series in ω_0, but for the present purpose the first term is all that is needed:

$$M = -k_3 \xi^4 H \omega_0 / (8\lambda_0^2) + \ldots, \tag{15}$$

where $$k_n = \int_0^\infty x^n f(x)\, \mathrm{d}x.$$

The Gibbs function relative to the normal state can now be calculated for unit length of the nucleus by substituting (9), (10) and (15) in (11)

$$\left.\begin{aligned} G_s(\omega_0, H) - G_n &= -A_c \omega_0, \\ \text{where} \quad A_c &= 2\pi k_1 \alpha \xi^2 - \frac{k_3 \xi^4 H^2}{16\lambda_0^2}. \end{aligned}\right\} \tag{16}$$

The thermodynamic condition favourable to the formation of this type of superconducting nucleus is that $A_c > 0$, or that

$$H^2 < \frac{32\pi k_1 \lambda_0^2 \alpha}{k_3 \xi^2}, \tag{17}$$

a condition which in general would be dependent on temperature, since α is dependent on temperature.

An analogous calculation can be made of the balance of the Gibbs function favourable to the formation of a single superconducting nucleus with spherical symmetry for which it is assumed that the variation of ω is still given by (9), where r is now the distance from the centre of the nucleus; the coefficient of ω_0 in the expression corresponding to (16) is given by

$$A_s = 4\pi k_2 \alpha \xi^3 - \frac{k_4 \xi^5 H^2}{12\lambda_0^2}, \tag{18}$$

and the condition for the stability of such a nucleus corresponding to (17) is that

$$H^2 < \frac{48\pi k_2 \lambda_0^2 \alpha}{k_4 \xi^2}. \tag{19}$$

So far the function f has been left unspecified, in the absence of any physical knowledge of its form; if, for example, $f(x) = \mathrm{e}^{-x^2}$ which mathematically is the most convenient function to choose for rough quantitative purposes, then

$$k_1 = \tfrac{1}{2}, \quad k_2 = \tfrac{1}{4}\pi^{\frac{1}{2}}, \quad k_3 = \tfrac{1}{2} \quad \text{and} \quad k_4 = \tfrac{3}{8}\pi^{\frac{1}{2}}. \tag{20}$$

The conditions (17) and (19) are then identical* and show that nuclei should be stable in fields less than a certain critical field H_c', where

$$H_c' = \frac{4\lambda_0 (2\pi\alpha)^{\frac{1}{2}}}{\xi}. \tag{21}$$

However, such nucleation will only be observed in practice if the full superconducting state does not supervene, or if $H_c' > H_c$. As we have seen, impure tin under certain conditions of temperature and field shows a behaviour symptomatic of nucleation. Experimentally it has been found that this occurs if l is less than a certain critical value l_c, which, considered in conjunction with (21), suggests a dependence of ξ on l. There must also be a variation of ξ with temperature, because, for most of the specimens, H_c/H_c' is almost independent of

* The use of (9) in defining the range of coherence ξ for cylindrical as well as spherical nuclei differs slightly from the concept of ξ used by Pippard (1955) in treating the trapping of flux in tin-indium alloys. There the spatial variation of ω is described by compounding spherically symmetrical functions.

PHILOSOPHICAL TRANSACTIONS OF THE ROYAL SOCIETY A MATHEMATICAL, PHYSICAL & ENGINEERING SCIENCES

temperature, as is exemplified by the results for specimen 4 shown in figure 12; by (21) this implies that ξ should have the same temperature variation as $\alpha^{\frac{1}{2}}/H_c$. A specific expression for α (and also for β) is given by the two-fluid phenomenological theory of Gorter & Casimir (1934), in which

$$\alpha = \frac{H_0^2}{8\pi}(1-t^2) \tag{22}$$

and

$$\beta = \frac{H_0^2 t^2}{16\pi}, \tag{23}$$

in the particular instance of a superconductor having a parabolic critical field curve

$$H_c = H_0(1-t^2). \tag{24}$$

With assumptions (22) and (24), which are only rough approximations for tin, the theory leading to (21) would represent the experimental observation (8) provided that ξ depends on l and t according to the relation

$$\xi = \frac{2\lambda_0 l}{l_c(1-t^2)^{\frac{1}{2}}}. \tag{25}$$

The penetration depth measured at the surface of pure tin is $5{\cdot}0\times10^{-6}$ cm; for tin with 3 % In it has risen to 10×10^{-6} cm, and is increasing quite rapidly with impurity (Pippard 1953). The quantity λ_0 occurring in the context of (25) may not necessarily be the same as the penetration depth so measured, but at least λ_0 is probably of the same order of magnitude as l_c, which we have seen to be approximately $8{\cdot}0\times10^{-6}$ cm (figure 13). It follows by (25) that ξ should be of the same order of magnitude as l at low temperatures, but should increase with temperature approaching T_c. According to the simple formula (25) ξ becomes infinite at T_c. Perhaps in reality it tends to a limiting value ξ_c. Yet we have seen, by considering the sharpness of transitions, that ξ_c must be more than 8 times greater than l for an impure specimen, while the absence of any experimental evidence for a quadratic relation such as (6)* between τ and H just below the transition temperature indicated that $\xi_c > 60l$. So the possibility must not be excluded that ξ tends to infinity as T approaches T_c.

Equation (8) defines a critical field curve of H_c' and t for the transition into a partially superconducting state, and is an idealization of the experimental results in so far as these show that in practice transitions occur over comparatively large intervals of temperature. However, the width of resistance transition is probably due to inhomogeneities in impurity concentration; such inhomogeneities in an annealed specimen would be of much larger dimensions than the radii ξ of superconducting nuclei, so that (8) might still be a valid condition for the abrupt establishment of an array of superconducting nuclei over regions small in comparison with the dimensions of the inhomogeneities. The conditions of field and temperature given by (8) for the establishment of partial superconductivity would, however, vary from one region of a specimen to another in correspondence with variations of the local value of l. In the course of any resistance transition, the different regions of a specimen should abruptly become partially superconducting (with local loss of resistance)

* It may be shown that (6) follows from the condition for the thermodynamic stability of a spherical superconducting nucleus; for (19) shows that over the small temperature range for which ξ may possibly have the constant value ξ_c, a field H would have the effect of depressing the reduced temperature of formation of a nucleus by τ, where

$$\tau = \frac{k_4 \xi_c H^2}{48\pi k_2 \lambda_0^2 (\partial\alpha/\partial\tau)}.$$

Here the approximation $\alpha = (\partial\alpha/\partial\tau)\,\tau$ is used. Equation (6) follows with the help of (20) and (22).

in the same order. The relation between the applied field H_c' and the reduced temperature t at which η takes a particular value should then give a critical field curve for a particular region of the specimen. Some support for this account of transition width is given by the results shown in figure 12 for specimen 4, which shows a behaviour typical of most of the specimens; it can be seen that the critical field curves obtained by the above procedure would show the same functional dependence of H_c' on t whether taken at $\eta = 0{\cdot}1$, $0{\cdot}5$ or $0{\cdot}9$. It follows that the points joined by erect lines in figure 13 represent the approximately temperature-independent ratios H_c/H_c' for different regions of a specimen having local values of l differing from the mean values calculated by (2) which are plotted as abscissae.

It can be shown, by arguments analogous to that used in considering the width of transitions in the absence of a field, that thermal fluctuations in T and ω probably play no important part in contributing to the width of transitions in the presence of fields.

(*b*) *The effect of current*

The results embodied in equation (7) and the figures of table 2 show that the current flowing through a specimen greatly influences the temperature of transition into the partially superconducting state. This effect may be due to the modification of the thermodynamic condition (17) or (19) for the inception of nucleation when account is taken of the kinetic energy of the supercurrent which flows through the nuclei. It is a consequence of the London electrodynamics that this kinetic energy is given by

$$F_j = \int \tfrac{1}{2}\Lambda j_s^2 \,\mathrm{d}v, \tag{26}$$

where the integration is over the volume of the superconducting phase.

In the simplest instance of a single cylindrically symmetrical filamentary nucleus alined in the direction of the applied field, a current i flowing along the length of the nucleus will be distributed radially to a first approximation in the same way as is ω (equation (9))

$$j_s = j_{s0} f\left(\frac{r}{\xi}\right), \tag{27}$$

where j_s is the paraxial component of the supercurrent density. This condition is, by (14), a consequence of the approximate constancy of the paraxial component of **A**. The free energy of the current i, given by (26), can then be integrated over unit length of a nucleus and can be shown by the use of (9), (13) and (27) to take the form $C_c i^2/\omega_0$, where $C_c = \lambda_0^2/k_1\xi^2$. The inclusion of this term in the expression (16) for the Gibbs function alters its character completely, since G does not now vary continuously as ω_0 rises from zero. It is therefore difficult to decide how to take into account the contribution of this additional kinetic energy. One might minimize G with respect to ω_0 and take as a criterion for the stability of the superconducting filament the condition that $G_s(\omega_0, H) - G_n$ shall not be positive; this leads to a depression of the temperature of nucleation which varies as $i^{\frac{2}{3}}$ rather than the experimentally observed $i^{\frac{1}{3}}$. The latter law occurs with such regularity in different specimens that it seems likely to be a genuine property of an impure superconductor, yet no simple explanation of it is forthcoming, and we are compelled to leave it as an unsolved problem. It is worth remarking, however, that the effect of current is of a magnitude that appears explicable only on the assumption that the filamentary nuclei are extremely sparsely distributed,

so that each must carry a substantial fraction of the current. An order of magnitude calculation indicates that perhaps only a fraction between 10^{-5} and 10^{-4} of the material is superconducting when the resistance has fallen to half its normal value. But whether this is really so, or whether the effect of current merely reveals a fundamental deficiency in the model employed for its analysis, is a question that must remain unanswered at present.

(*c*) *Relevance to existing phenomenological theories of superconductivity*

No account is taken of the effect of electronic scattering in either the London electrodynamics or the phenomenological theory of Ginsburg & Landau (1950). In the latter theory, inclusion of a term in the free energy dependent on the gradient of ω gives rise to a long-range ordering of the superconducting phase. On account of the neglect of scattering the theory is not immediately applicable to impure superconductors; for a straightforward addition of the extra term to the Gibbs function (16) of a cylindrical nucleus has the effect of making the conditions of nucleation unrealizable. It is clear that whatever truth this theory may have when applied to pure superconductors, the extra free energy associated with gradients of ω must be substantially reduced by the addition of impurities.

The expression (25) for the range of coherence ξ bears a close resemblance to that suggested for a similar quantity in Pippard's phenomenological theory of superconductivity (1953). In this theory the local relationship (12) or (14) between $\mathbf{j}_s$ and $\mathbf{A}$ is replaced by a non-local relationship in which the range of coherence ξ appears as a measure of the range over which $\mathbf{A}$ must be averaged in determining the supercurrent at a point. The theory is developed for the particular condition of constant ω. In the present context ξ is introduced in (9), in what is probably an equivalent manner, as being the least range over which ω is capable of substantial variation. The variation of penetration depth with impurity observed by Pippard is shown to be reproduced by the theory if ξ at 0° K is taken to be nearly equal to the mean free path l, as is so in order of magnitude in (25). The temperature variation of ξ is suggested to be as $(1-t^4)^{-\frac{1}{2}}$; the factor $(1-t^2)^{-\frac{1}{2}}$ occurs in (25), but the consistency of the present results is not sufficient to distinguish between these forms of variation. It seems probable therefore that it is the same quantity ξ which appears in both contexts.

The operation of a non-local relationship between $\mathbf{j}_s$ and $\mathbf{A}$ would to a certain extent invalidate the calculation of the conditions for nucleation based on the local relationship (14), and since also the choice of e^{-x^2} for the function $f(x)$ is arbitrary, no exactness is to be expected in the numerical factor entering into (25). In addition λ_0, as it appears in the condition for nucleation (21), may not necessarily be the same quantity as the penetration depth measured at the surface of impure tin. Pippard's theory gives this penetration depth $\lambda_0 \propto \xi^{-\frac{1}{3}}$ for very impure tin, and if $\xi \propto l$ it would follow by substitution into (21) that $H_c/H_c' \propto l^{\frac{2}{3}}$. This dependence would not give so adequate a representation of the experimental results in figure 13 as does the proportionality of H_c/H_c' to l indicated there which would hold were λ_0 independent of l. The experimental results, however, are not conclusive on this point, nor do they permit a distinction to be made between a simple proportionality of ξ and l and an alternative relation considered by Pippard:

$$1/\xi = 1/\xi_0 + 1/\alpha l,$$

where ξ_0 is of the order of 10^{-4} cm, and α a numerical constant of order unity.

It is clear that the concept of a range of coherence ξ as formulated in Pippard's phenomenological theory yields an adequate account of the general characteristics of the partially superconducting state found in tin-indium alloys, although a detailed account is not yet possible. The large width of resistance transitions to the partially superconducting state, even in the absence of a field for the most impure specimens, and perhaps also the large effect of current on the transitions, suggest that even a careful method of preparation of the specimens has not entirely removed the influence of inhomogeneities and lattice imperfections. Nevertheless, it does not seem unreasonable to believe that they do no more than obscure the characteristic behaviour of homogeneous superconducting alloys and that the observed effects are in the main susceptible of a simple description in terms of a range of coherence, dependent on temperature and on the density of centres of electronic scattering.

I wish to thank Dr D. Shoenberg, F.R.S., for his interest in the work; Dr A. B. Pippard originally suggested the experiments, and I am most grateful to him for invaluable guidance and encouragement. The work was carried out during the tenure of an award from the Department of Scientific and Industrial Research.

References

Bridgman, P. W. 1928 *Proc. Amer. Acad. Arts Sci.* **63**, 351.
Chambers, R. G. 1952 *Proc. Roy. Soc.* A, **215**, 481.
Ginsburg, V. L. & Landau, L. D. 1950 *J. Exp. Theor. Phys. U.S.S.R.* **20**, 1064.
Gorter, C. J. & Casimir, H. B. G. 1934 *Z. tech. Phys.* **12**, 539.
de Haas, W. J. & Voogd, J. 1931 *Commun. Phys. Lab. Univ. Leiden*, no. 214*c*.
Kapitza, P. & Milner, C. J. 1937 *J. Sci. Instrum.* **14**, 5.
Kok, J. A. 1934 *Physica*, **1**, 1103.
Lock, J. M., Pippard, A. B. & Shoenberg, D. 1951 *Proc. Camb. Phil. Soc.* **47**, 811.
Mendelssohn, K. 1935 *Proc. Roy. Soc.* A, **152**, 34.
Pippard, A. B. 1950 *Proc. Roy. Soc.* A, **203**, 210.
Pippard, A. B. 1951 *Proc. Camb. Phil. Soc.* **47**, 617.
Pippard, A. B. 1952 *Phil. Mag.* **43**, 273.
Pippard, A. B. 1953 *Proc. Roy. Soc.* A, **216**, 547.
Pippard, A. B. 1955 *Phil. Trans.* A, **248**, 97.
Serin, B. & Lohman, C. 1954 *Proc. Third Int. Conf. Low Temp. Phys.* (*Houston*), p. 47.
Shoenberg, D. 1952 *Superconductivity*, p. 37. Cambridge University Press.

PHILOSOPHICAL TRANSACTIONS OF THE ROYAL SOCIETY A MATHEMATICAL, PHYSICAL & ENGINEERING SCIENCES